AIP | Physics of Plasmas

Space charge effects in rf traps: Ponderomotive concept and stroboscopic analysis

Kushal Shah and Harishankar Ramachandran

Citation: Physics of Plasmas (1994-present) **16**, 062307 (2009); doi: 10.1063/1.3152326
View online: http://dx.doi.org/10.1063/1.3152326
View Table of Contents: http://scitation.aip.org/content/aip/journal/pop/16/6?ver=pdfcov
Published by the AIP Publishing

Space charge effects in rf traps: Ponderomotive concept and stroboscopic analysis

Kushal Shah[a] and Harishankar Ramachandran[b]
Department of Electrical Engineering, Indian Institute of Technology Madras, Chennai 600036, India

(Received 19 March 2009; accepted 18 May 2009; published online 10 June 2009)

Exact solutions for one-dimensional (1D) plasma dynamics in an rf trap are known when space charge effects are neglected [K. Shah and H. S. Ramachandran, Phys. Plasmas **15**, 062303 (2008)]. In this work, weak space charge effects in an rf trap are considered. An analytic expression for the time varying distribution function of the 1D plasma is obtained. It is shown that the plasma is a Maxwellian up to the lowest order in nonlinearity and that the spatially constant temperature periodically oscillates in time at the same rate as the rf frequency. It was shown by Krapchev [Phys. Rev. Lett. **42**, 497 (1979)] that the time averaged distribution function is double humped with respect to velocity beyond a certain threshold in space. The time average of the complete time varying distribution function is obtained and some of the predictions of Krapchev are recovered, while also finding discrepancies. The relationship between stroboscopic orbits and the time averaged ponderomotive orbit are obtained for such traps. © *2009 American Institute of Physics*.
[DOI: 10.1063/1.3152326]

I. INTRODUCTION

The response of a plasma to a nonuniform oscillating electric field has been of considerable interest in rf traps.[1–6] Usually, such fields have both a dc and a high frequency component. In one dimension, such a field is given by

$$E(x,t) = h(x) + g(x)\cos(\omega t), \tag{1}$$

where $h(x)$ and $g(x)$ are smooth but otherwise arbitrary functions of the spatial coordinate and ω is the frequency of oscillations. The response of plasma to fields of the above kind is characterized by the well known ponderomotive effect.[7–11]

The path of the particles under a force of the form in Eq. (1) will have a low magnitude high frequency component superimposed on a drift component. Using first order time averaging techniques,[12–15] it can be shown that the equation representing the drift motion of the particles will be given by

$$\ddot{x}_a = - \left. \frac{d\phi_p(x)}{dx} \right|_{x=x_a}, \tag{2}$$

where ϕ_P is the fictitious ponderomotive potential given by

$$\phi_P = \phi_0(x) + \frac{e^2}{4m^2\omega^2} g^2(x),$$

where e is the charge and m the mass of the particle and $\phi_0(x)$ is the static potential energy of the particles corresponding to the dc field, $h(x)$. It is widely accepted[9,16] that the time averaged density of the plasma under a field given by Eq. (1) will be

$$n = n_0 \exp\left(-\frac{\phi_P}{T_0}\right), \tag{3}$$

where n_0 is the density where $\Phi_p = 0$ and T_0 is the temperature. Equation (3) also follows from the conjecture that the time averaged distribution function of the plasma is constant on curves of time averaged motion of the individual particles. Ponderomotive theory is used to study phenomenon like laser wake field acceleration[17–19] and interaction of Langmuir waves with ion-acoustic waves in the context of Zakharov equation.[20]

The special case when $g(x)$ and $h(x)$ are proportional to x has applications in $2d$ linear rf traps,[21,22] $3d$ ion traps,[1] and combined rf traps.[23–25] The linear rf trap and ion trap are mechanisms for confining single species plasma, widely used in mass spectroscopy,[26] and also have applications in areas like quantum information[27] where a single or very few charged particles have to be trapped. The combined rf trap is used to trap two different charged species of widely varying masses in the same region of space and is mainly used in antihydrogen production. These traps take advantage of the fact that the boundedness of particle orbits in a linearly varying rf field is independent of the initial conditions. It only depends on the applied field strength. However, nonlinearity could arise in the field from two different sources. First, the externally applied field itself is not exactly linear for any real experiment. There are octopole and higher order terms. Second, the trapped particles themselves induce a space-charge field whose profile is nonlinear.

In an earlier work,[28] the authors considered the linear field case and obtained exact analytic expressions for the one-dimensional distribution function and density of the plasma. Space charge effects and other sources of nonlinearity were neglected. The analysis showed that the correct expression for the time averaged plasma density differs from the expression given in Eq. (3) even to first order. In this

[a]Electronic mail: atmabodha@gmail.com.
[b]Electronic mail: hsr@ee.iitm.ac.in.

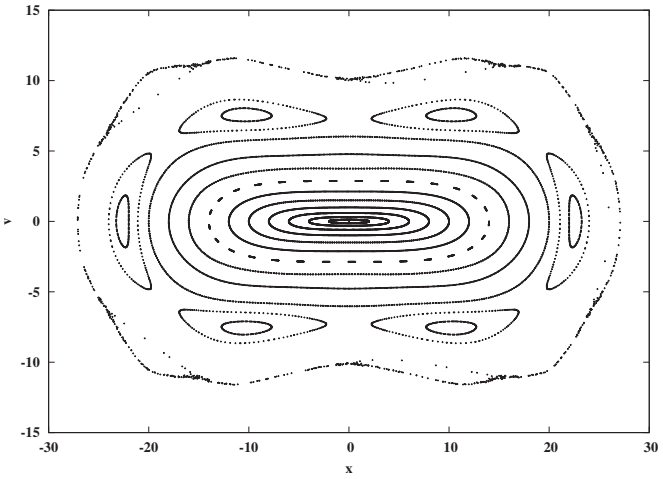

FIG. 1. This figure shows the stroboscopic plot of the phase space trajectory of particles with different initial conditions under the force equation given by Eq. (8) keeping terms up to $\mathcal{O}(q^2)$. It can be seen that some orbits are simple closed curves and some orbits form islands in phase space. The numerical values of the various parameters were $p_e=-0.01$, $q_e=0.16\approx q$, $\omega_p=0.5\nu_0$, and $\bar{x}=1$.

work, we extend our earlier work by including the effects of space charge of the plasma trapped in rf traps and obtain analytic expressions for the distribution function of the plasma up to the lowest order in plasma density. These expressions again lead to an expression for the time averaged plasma density that differs from Eq. (3).

When characterizing particle motion under the effect of nonlinear electric fields, some important considerations are whether the orbits are regular or chaotic and whether we can solve for the particle trajectories as functions of time. Figure 1 shows stroboscopic plots of the particle orbits for the fields given by Eq. (1), with $g(x)$ being proportional to x and $h(x)$ having a cubic nonlinearity. As can be seen, some initial conditions lead to simple closed curves and some others result in a chain of islands. The particle paths corresponding to these initial conditions are regular.[29] There are also initial conditions for which the stroboscopic plot fills an area in phase space. These plots correspond to particle orbits that are chaotic. Regions in phase space where the stroboscopic plot changes from being a simple closed curve to a chain of islands are a site for chaos. For regions in phase space where the stroboscopic plots are simple closed curves, one could employ the multiple scale analysis used in solving standard Mathieu's equation to solve for the case of nonlinear dc fields as well.[30]

In order to study the statistical properties of the plasma in a rf trap and also to find the time averaged density, it is necessary to solve for the plasma distribution function, $f(x,v,t)$. For collisionless plasmas, this function is a solution of the Vlasov equation[7,31] and is constant on the individual particle paths ($df/dt=0$ even though $\partial f/\partial t\neq 0$). Thus, after having obtained analytic expressions for the particle paths, it is important to solve for the corresponding invariant. Given any arbitrary specification of electric field, the initial conditions of the particle, namely, the initial position and velocity, are certainly two invariants. Any arbitrary combination of these two fundamental invariants is also an invariant.[32] Since the applied field is time varying, none of these invariants can be time independent. However, since the field is time periodic, it is reasonable to expect the distribution function to be periodic at any fixed point in phase space and with the same time period as the applied field. As we will show in this paper, analytic expressions for such a ω-invariant distribution function can be obtained for regions in phase space where the stroboscopic plot of the particle trajectory is a simple closed curve.

Another issue of importance in an actual rf trap experiment is the maximum amount of plasma that can be trapped. This depends on the parameters of the applied field. From the point of view of ponderomotive theory, it is easy to show that the plasma frequency, $\omega_p=\sqrt{4\pi n_0 e^2/m}$, must be less than the slow frequency, ν_0, that characterizes the drift motion of the particles. Consider plasma trapped by rf fields. The time averaged plasma density contributes to a repulsive force on particles given by

$$\frac{e}{m}E_x(x)=\int_0^x \omega_p^2 dx' \simeq \omega_p^2 x$$

for a nearly uniform density profile. Given a trap characterized by

$$\frac{e}{m}E_{\mathrm{ext},x}(x)=(-p_e+2q_e\cos 2t)x,$$

the space charge adds to the dc field to yield the following orbit equation,

$$\ddot{x}=(-p_e+\omega_p^2+2q_e\cos 2t)x.$$

From Eq. (2) we know that ponderomotive theory turns this into the following equation in slow time:

$$\ddot{x}_a=\left(-p_e+\omega_p^2-\frac{q_e^2}{2}\right)x_a. \tag{4}$$

Thus, for stable orbits, the plasma frequency must be bounded above by $\nu_0=\sqrt{p_e+0.5q_e^2}$. This is exactly what is observed in experiments where the maximum plasma frequency is found to be close to ν_0.[33] Experiments also observed that the plasma profile is approximately Gaussian in shape,[34] which is what is expected in the presence of a parabolic confining potential. These ideas that are based on naive ponderomotive theory are given a more rigorous treatment in the rest of this paper.

The results of this paper fall into two categories. There are results that describe the self-consistent response of the plasma to an rf field. There are also results that describe the (non-self-consistent) plasma response for a given total electric field. The two sets of results are valid over different ranges of phase space, but both are important as the latter results are important when comparing with literature where computations are only for the plasma response to a prescribed electric field.

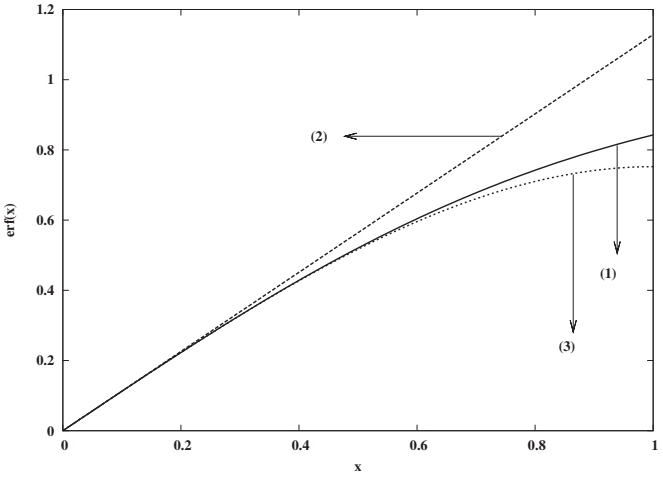

FIG. 2. This is a plot of the error function. Curve (1) shows the exact error function. Curve (2) is the linear approximation and curve (3) is the plot with the cubic nonlinearity taken in. This shows that $2(x-x^3/3)/\sqrt{\pi}$ is a good approximation to the exact error function, erf(x), up to $x=1$.

The following sections are organized as follows. In Sec. II, we obtain the modified force equation when space charge effects are taken into account and then solve this force equation. The time averaged expressions of these solutions are then compared with the predictions of conventional ponderomotive theory. Then in Sec. III, we obtain expressions for the ω-invariant distribution function and the plasma density. Section IV discusses these results and Sec. V contains conclusions.

II. THE FORCE EQUATION AND ITS SOLUTIONS

In a rf trap, the applied field is linear. The equation of motion of charged particles under such a field is $\ddot{x}=[-p_e+2q_e\cos(2\tau)]x$, where p_e and q_e are the normalized dc and rf field strengths, respectively, and $\tau=\omega t/2$ is the normalized time. The distribution function of the plasma under such a field can be exactly solved for.[29] Using these exact solutions, it has been shown in our earlier work that the field induced by the charged particles (charge e and mass m) is

$$E_i(x,\tau)=2\pi e n_0\sqrt{\frac{\pi}{\beta_0\gamma_0}}\mathrm{erf}\left\{\frac{x}{\bar{x}}\left[1+\frac{q_e}{2}\cos 2\tau+\mathcal{O}(q_e^2)\right]\right\}, \tag{5}$$

where $1/\beta_0$ is the initial temperature of the plasma, $\gamma_0\approx 0.5\nu_0^2(1+2q)$, and $\bar{x}\approx 1/\sqrt{\beta_0\gamma_0}$. Equation (5) can be Taylor expanded in x to get

$$\frac{eE_i}{m}=\omega_p^2\left[1+\frac{q_e}{2}\cos 2\tau\right]x-\frac{\omega_p^2}{3\bar{x}^2}\left[1+\frac{3q_e}{2}\cos 2\tau\right]x^3+\cdots \tag{6}$$

The first term on the right is the way the space charge modifies the externally applied linear electric field. As can be seen, there is both a change in the dc field and a change in rf confining field. Thus, the first term on the right merely modifies the strength of the applied field without modifying its shape. The second term is the first nonlinear factor and is proportional to x^3. In Fig. 2, curve (3) is the cubic approximation to the error function, erf$(x/\bar{x})$. Since it is a good approximation right out to $x=\bar{x}$, Eq. (6) is a suitable description of the plasma response to the applied field in the bulk region of the plasma. Thus, the first nonlinearity to appear in Eq. (5) due to space charge effects is of the order of x^3. Taking into account this cubic nonlinearity, the modified equation for the motion of an ion in the rf trap takes the form

$$\frac{d^2x}{d\tau^2}+px=2qx\cos 2\tau-\frac{\omega_p^2}{3}\left(\frac{x}{\bar{x}}\right)^2x-q\frac{\omega_p^2}{2}\left(\frac{x}{\bar{x}}\right)^2x\cos 2\tau, \tag{7}$$

where $p=p_e-\omega_p^2$ and $q=q_e(1+0.25\omega_p^2)\approx q_e$ since $\omega_p\ll\omega=2$. As can be seen from Eq. (7), the $qx^3\cos 2\tau$ term is of a higher order than the x^3 term since $q\ll 1$. It is worth noting that q is of the order of unity in typical experiments; however, theoretical treatments can make progress only when q is assumed to be a small parameter. We will assess the importance of neglected terms in real experimental conditions later in Sec. IV. Neglecting the $qx^3\cos 2\tau$ term in Eq. (7), we obtain

$$\frac{d^2x}{d\tau^2}+px=2qx\cos 2\tau-q^2\alpha x^3, \tag{8}$$

where $q^2\alpha=\omega_p^2/3\bar{x}^2$. Equation (8) can be solved by using the multiple scale analysis method used to solve Mathieu's equation.[35] The solutions of Eq. (8), up to $\mathcal{O}(q^2)$, are found to be [Appendix A (Ref. 36)]

$$\begin{aligned}x(\tau)=&A\cos(\nu\tau+\phi)\\&-\frac{qA}{4}\left[\frac{\cos(\nu\tau+2\tau+\phi)}{1+\nu}+\frac{\cos(\nu\tau-2\tau+\phi)}{1-\nu}\right]\\&+\frac{q^2A}{32}\left[\frac{\cos(\nu\tau+4\tau+\phi)}{(1+\nu)(2+\nu)}+\frac{\cos(\nu\tau-4\tau+\phi)}{(1-\nu)(2-\nu)}\right]\\&-\frac{q^2\alpha A^3}{4}\frac{\cos(3\nu\tau+3\phi)}{-8\nu^2},\end{aligned} \tag{9}$$

$$\begin{aligned}v(\tau)=&-\nu A\sin(\nu\tau+\phi)-\frac{qA}{4}\left[\frac{(\nu+2)\sin(\nu\tau+2\tau+\phi)}{1+\nu}\right.\\&\left.+\frac{(\nu-2)\sin(\nu\tau-2\tau+\phi)}{1-\nu}\right]\\&-\frac{q^2A}{32}\left[\frac{(\nu+4)\sin(\nu\tau+4\tau+\phi)}{(1+\nu)(2+\nu)}\right.\\&\left.+\frac{(\nu-4)\sin(\nu\tau-4\tau+\phi)}{(1-\nu)(2-\nu)}\right]\\&+3\nu\frac{q^2\alpha A^3}{4}\frac{\sin(3\nu\tau+3\phi)}{-8\nu^2},\end{aligned} \tag{10}$$

with

$$\nu^2 = p + \frac{q^2}{2} + \frac{3\alpha q^2 A^2}{4}. \tag{11}$$

Equation (11) shows that under the effect of the nonlinear space charge field, the slow frequency of the particles depends on oscillation amplitude and is no longer a constant as was the case of purely linear fields.

As mentioned before, Equations such as Eq. (1), which belong to the category of equations where a high frequency forcing function is present, are usually analyzed by using the theory of averaging. Time averaging the expressions for $x(t)$ and $v(t)$ given in Eqs. (9) and (10) [Appendix B (Ref. 36)] yields

$$\begin{aligned} x_a(\tau) &= \frac{1}{\pi}\int_{\tau-\pi/2}^{\tau+\pi/2} x(t)dt \\ &\approx A\cos(\nu\tau+\phi) + \frac{q^2\alpha A^3}{32\nu^2}\cos(3\nu\tau+3\phi), \\ v_a(\tau) &= \frac{1}{\pi}\int_{\tau-\pi/2}^{\tau+\pi/2} v(t)dt \\ &\approx -\nu A\sin(\nu\tau+\phi)\frac{2\sin(\nu\pi/2)}{\nu\pi} \\ &\quad -\frac{3q^2\alpha A^3}{32\nu}\sin(3\nu\tau+3\phi), \end{aligned} \tag{12}$$

where the residual high-frequency ripple has been neglected. Additionally, a factor $2\sin(\nu\pi/2)/\nu\pi$ has been dropped from the first time on the right side of the equations. This is because the second terms on the right side of Eqs. (A2) and (A3) in Appendix A (Ref. 36) suffer from the problem of small denominators and those terms are actually of the order of $q^2\alpha A^2/\nu^2$ compared to the first term. Using Eq. (8) with $A=\mathcal{O}(\bar{x})$, this is of the order of ω_p^2/ν^2 and hence of the order of unity by Eq. (4). Thus, these terms have to be taken into account. The factor of $2\sin(\nu\pi/2)/\nu\pi$ that multiplies the leading terms is, thus, a higher order correction.

The time averaged response to Eq. (8) is conventionally obtained by averaging the Hamiltonian. The time averaged ponderomotive Hamiltonian for this equation is given by

$$H_p = \frac{v^2}{2} + \frac{px^2}{2} + \frac{q^2x^2}{4} + \frac{q^2\alpha x^4}{4}. \tag{13}$$

The particle orbits corresponding to Eq. (13), obtained by a perturbation analysis,[37] are found to be

$$\begin{aligned} x_p(\tau) &\approx A_p\cos(\nu\tau+\phi_p) + \frac{q^2\alpha A_p^3}{32\nu^2}\cos(3\nu\tau+3\phi_p), \\ v_a(\tau) &\approx -\nu A_p\sin(\nu\tau+\phi_p) - \frac{3q^2\alpha A_p^3}{32\nu}\sin(3\nu\tau+3\phi_p), \end{aligned} \tag{14}$$

which is the same as the expressions for time averaged orbits, Eq. (12). It must be noted that the derivation of the ponderomotive Hamiltonian includes the notion of averaging over a "fast period," but no $\sin\nu\pi/\nu\pi$ term appears due to the implicit assumption that $\nu\to 0$.

III. PLASMA DISTRIBUTION FUNCTION

For collisionless plasmas, the distribution function is simply a function of any invariant associated with single particles. For periodically driven systems, it is reasonable to expect such a function to be invariant on the same time scale, $2\pi/\omega$, as the driving force. For a given time varying nonlinear electric field, such an ω-invariant distribution will exist only if the stroboscopic plot of the orbits in phase space are simple closed curves.

A stroboscopic plot of the particle orbit leads to a countable subset of discrete points, separated by fixed time intervals of $2\pi/\omega=\pi$, on the phase space orbit. The numerical analysis of Eq. (8) shows that the stroboscopic plot of the particle orbit is dense on a simple closed curve only where the gradients in the field are small enough. This can be seen in Fig. 1. For other regions in phase space, we see island structures and, possibly, chaos. Analytic expressions for the distribution function can only be expected to hold in the regular region and, thus, we cannot expect a global distribution function for the entire phase space that is ω-invariant. However, in regions of phase space where the stroboscopic plot yields a simple closed curve, such a function can be obtained. Such curves correspond to an irrational value of the slow frequency ν. Of course, every rational value of ν even in these regions results in island formation. However, their widths are so small that their effect on the dynamics is negligible.

Figure 3 shows the particle orbit (curve 1) together with the stroboscopic curve (curve 2). The time averaged orbit (curve 3) is also shown for reference. It is clear that the actual orbit differs considerably from the stroboscopic curve. An odd aliasing effect is also seen in the stroboscopic curve in that it touches the actual orbit at different phases of the fast oscillation at different slow times. This results in a curve that differs from the time averaged curve shown in the figure, even though both have the same shape up to $\mathcal{O}(q^2)$.

If we start from a time τ and sample the particle orbit at equal time steps of $2\pi/\omega=\pi$, this is equivalent to replacing τ in Eqs. (9) and (10) by $\tau+n\pi$, where $n\in\mathcal{Z}$. As shown in Appendix C,[36] this leads to analytic expressions for the stroboscopic points,

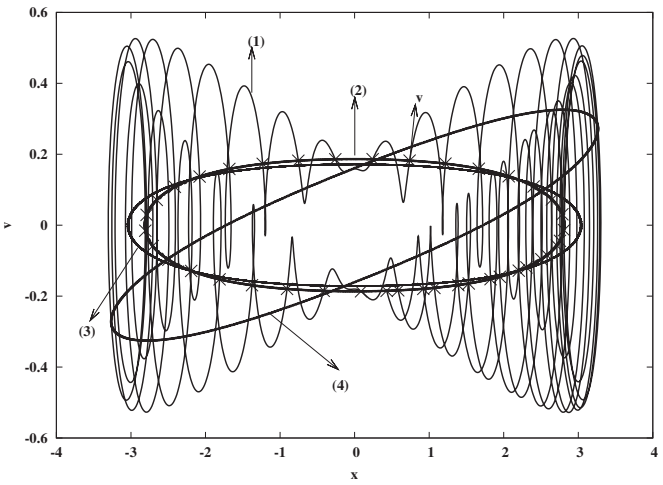

FIG. 3. This plot shows the stroboscopic map of the particle orbits in phase space. Curve (1) is the full orbit as obtained by integration of Eq. (8). Curve (2) is the stroboscopic plot obtained by a sampling of the particle orbit at a fixed time step of $2\pi/\omega$ starting from $\tau=0$. The big crosses correspond to a few points on this level curve. These points form a countable set that is dense on the level curve given by Eq. (21). Curve (3) is the time averaged orbit and corresponds to the time averaged ponderomotive Hamiltonian, Eq. (13). Curve (4) is also a stroboscopic plot like curve (2), but, in this case, the sampling begins at $\tau \neq 0$. The arrow labeled v shows the direction of sampled velocity, v_s, at one particular instant of time. It can be clearly seen that v_s is not along the stroboscopic level curve, which explains the reason why $v_s \neq dx_s/dt$ in Eqs. (16) and (17).

$$
\begin{aligned}
x(\tau+n\pi) = &\left[A - \frac{qA}{2}\frac{\cos(2\tau)}{1-\nu^2}\right.\\
&\left.+\frac{q^2A}{16}\frac{(2+\nu^2)\cos(4\tau)}{[1-\nu^2][2-\nu^2]}\right]\cos(\nu\tau+\nu n\pi+\phi)\\
&\times\left[-\frac{qA}{2}\frac{\nu\sin(2\tau)}{1-\nu^2}\right.\\
&\left.+\frac{q^2A}{16}\frac{3\nu\sin(4\tau)}{[1-\nu^2][2-\nu^2]}\right]\sin(\nu\tau+\nu n\pi+\phi)\\
&-\frac{q^2\alpha A^3}{4}\frac{\cos(3\nu\tau+3\nu\tau_s+3\phi)}{-8\nu^2},
\end{aligned}
\tag{15}
$$

$$
\begin{aligned}
v(\tau+n\pi) = &\left[-\nu A + \frac{qA}{2}\frac{-\nu\cos(2\tau)}{1-\nu^2}\right.\\
&\left.-\frac{q^2A}{16}\frac{(\nu^3-10\nu)\cos(4\tau)}{[1-\nu^2][2-\nu^2]}\right]\sin(\nu\tau+\nu n\pi+\phi)\\
&+\left[\frac{qA}{2}\frac{(2-\nu^2)\sin(2\tau)}{1-\nu^2}\right.\\
&\left.-\frac{q^2A}{16}\frac{(8+\nu^2)\sin(4\tau)}{[1-\nu^2][2-\nu^2]}\right]\cos(\nu\tau+\nu n\pi+\phi)\\
&+3\nu\frac{q^2\alpha A^3}{4}\frac{\sin(3\nu\tau+3\nu\tau_s+3\phi)}{-8\nu^2}.
\end{aligned}
$$

Since the stroboscopic points, $x(\tau+n\pi)$ and $v(\tau+n\pi)$, are dense on a simple closed curve in phase space, we can also define a continuous time τ_s on these level curves of the stroboscopic map. This allows us to determine the invariant underlying the curve. As shown in Appendix C,[36] the continuous time expressions for stroboscopic coordinates (x_s, v_s) in phase space are given by replacing $n\pi$ by τ_s in Eq. (15),

$$
\begin{aligned}
x_s(\tau+\tau_s) = &\left[A - \frac{qA}{2}\frac{\cos(2\tau)}{1-\nu^2}\right.\\
&\left.+\frac{q^2A}{16}\frac{(2+\nu^2)\cos(4\tau)}{[1-\nu^2][2-\nu^2]}\right]\cos(\nu\tau+\nu\tau_s+\phi)\\
&\times\left[-\frac{qA}{2}\frac{\nu\sin(2\tau)}{1-\nu^2}\right.\\
&\left.+\frac{q^2A}{16}\frac{3\nu\sin(4\tau)}{[1-\nu^2][2-\nu^2]}\right]\sin(\nu\tau+\nu\tau_s+\phi)\\
&-\frac{q^2\alpha A^3}{4}\frac{\cos(3\nu\tau+3\nu\tau_s+3\phi)}{-8\nu^2},
\end{aligned}
\tag{16}
$$

$$
\begin{aligned}
v_s(\tau+\tau_s) = &\left[-\nu A + \frac{qA}{2}\frac{-\nu\cos(2\tau)}{1-\nu^2}\right.\\
&\left.-\frac{q^2A}{16}\frac{(\nu^3-10\nu)\cos(4\tau)}{[1-\nu^2][2-\nu^2]}\right]\sin(\nu\tau+\nu\tau_s+\phi)\\
&+\left[\frac{qA}{2}\frac{(2-\nu^2)\sin(2\tau)}{1-\nu^2}\right.\\
&\left.-\frac{q^2A}{16}\frac{(8+\nu^2)\sin(4\tau)}{[1-\nu^2][2-\nu^2]}\right]\cos(\nu\tau+\nu\tau_s+\phi)\\
&+3\nu\frac{q^2\alpha A^3}{4}\frac{\sin(3\nu\tau+3\nu\tau_s+3\phi)}{-8\nu^2}.
\end{aligned}
\tag{17}
$$

Here, for $\tau_s=0$, $x_s(\tau)$, and $v_s(\tau)$ are points on the continuous orbit. For fixed τ, $x_s(\tau+\tau_s)$ and $v_s(\tau+\tau_s)$ trace out the stroboscopic curve passing through that phase space point, $x_s(\tau), v_s(\tau)$. $v_s(\tau+\tau_s)$, the instantaneous velocity at a stroboscopic point (shown in Fig. 3 by an arrow), is clearly not along the stroboscopic plot, i.e., $v_s \neq dx_s/d\tau_s$. Hence, for fixed τ, the stroboscopic coordinates, (x_s, v_s), as functions of τ_s, are not the spatial coordinate and velocity in the usual sense.

To obtain the ω-invariant energy expression (periodic in τ) for the actual particle orbit, we need to eliminate τ_s from Eqs. (16) and (17). For $\tau=0$, $x_s(\tau_s)$ and $v_s(\tau_s)$ can be simply scaled to obtain the same expressions as Eq. (12). Hence, a scaled version of Eq. (13) represents the invariant for these stroboscopic level curves corresponding to $\tau=0$. As shown in Appendix D,[36] for $\tau>0$, a simple rotation and scaling again reduces $x_s(\tau+\tau_s)$ and $v_s(\tau+\tau_s)$ to the expressions in Eq. (12)

$$
\begin{aligned}
X &= A\cos(\nu\tau+\nu\tau_s+\phi)+\frac{q^2\alpha A^3}{32\nu^2}\cos(3\nu\tau+3\nu\tau_s+3\phi)V\\
&= -\nu A\sin(\nu\tau+\nu\tau_s+\phi)\\
&\quad-\frac{3q^2\alpha A^3}{32\nu}\sin(3\nu\tau+3\nu\tau_s+3\phi),
\end{aligned}
\tag{18}
$$

where $X=[x_s+q(c_2/c_3)v_s]/[c_1+q^2(c_2c_4/c_3)]$ and $V=[v_s-q(c_4/c_1)x_s]/[c_3+q^2(c_2c_4/c_1)]$, and c_1, c_2, c_3, and c_4 are periodic functions of τ with the same period as the rf field,

$2\pi/\omega$. Comparing Eq. (18) to Eq. (12), it is clear that $X(\tau+\tau_s)=x_a(\tau+\tau_s)$ and $V(\tau+\tau_s)=v_a(\tau+\tau_s)$ to $\mathcal{O}(q^2)$. Thus the dynamical structure connecting X and V is the same as that governing x_a and v_a, i.e., the ponderomotive Hamiltonian, Eq. (13). This leads to an expression for the ω-invariant energy,

$$E_\omega(x,v,\tau)=\frac{V^2}{2}+\frac{pX^2}{2}+\frac{q^2X^2}{4}+\frac{q^2\alpha X^4}{4}$$
$$=\frac{1}{2}\left(\frac{v_s-q\dfrac{c_4(\tau)}{c_1(\tau)}x_s}{\left[c_3(\tau)+q^2\dfrac{c_2(\tau)c_4(\tau)}{c_1(\tau)}\right]}\right)^2+\frac{1}{2}\left(p+\frac{q^2}{2}\right)$$
$$\times\left(\frac{x_s+q\dfrac{c_2(\tau)}{c_3(\tau)}v_s}{\left[c_1(\tau)+q^2\dfrac{c_2(\tau)c_4(\tau)}{c_3(\tau)}\right]}\right)^2$$
$$+\frac{q^2\alpha}{4}\left(\frac{x_s+q\dfrac{c_2(\tau)}{c_3(\tau)}v_s}{\left[c_1(\tau)+q^2\dfrac{c_2(\tau)c_4(\tau)}{c_3(\tau)}\right]}\right)^4. \quad (19)$$

Keeping only terms up to $\mathcal{O}(q^2)$, the expression for ω-invariant energy corresponding to Eq. (8) is given by

$$E_\omega(x,v,\tau)=\frac{1}{2}\left(\frac{v-q\dfrac{c_4(\tau)}{c_1(\tau)}x}{\left[c_3(\tau)+q^2\dfrac{c_2(\tau)c_4(\tau)}{c_1(\tau)}\right]}\right)^2+\frac{1}{2}\left(p+\frac{q^2}{2}\right)$$
$$\times\left(\frac{x}{\left[c_1(\tau)+q^2\dfrac{c_2(\tau)c_4(\tau)}{c_3(\tau)}\right]}\right)^2$$
$$+\frac{q^2\alpha}{4}\left(\frac{x}{\left[c_1(\tau)+q^2\dfrac{c_2(\tau)c_4(\tau)}{c_3(\tau)}\right]}\right)^4. \quad (20)$$

It should be noted that $E_\omega(x,v,\tau)$ is invariant over the detailed orbit (curve 1) in Fig. 3. For time instants $\tau=n\pi$, the above expression for the ω-invariant energy becomes

$$E_\omega(x,v,\tau=n\pi)=\frac{1}{2}\left(\frac{v}{1+0.5q-0.3125q^2}\right)^2+\frac{1}{2}\left(p+\frac{q^2}{2}\right)$$
$$\times\left(\frac{x}{1-0.5q+0.0625q^2}\right)^2$$
$$+\frac{q^2\alpha}{4}\left(\frac{x}{1-0.5q+0.0625q^2}\right)^4. \quad (21)$$

As can be clearly seen, the above equation is a scaled version of the time averaged ponderomotive Hamiltonian, Eq. (13).

In principle, any function of $E_\omega(x,v,\tau)$ is an ω-invariant distribution function of the plasma under the effect of the force equation, Eq. (8). Since E_ω is quadratic in v, a distribution of the form

$$f(x,v,\tau)=n_0\sqrt{\frac{1}{2\pi T_0}}\exp\left(-\frac{E_\omega(x,v,\tau)}{T_0}\right) \quad (22)$$

has a velocity distribution that is Maxwellian at every point. Here, E_ω is given by Eq. (20) and n_0 and T_0 are the density and temperature, respectively, at the origin. Since this distribution function is Maxwellian [up to $\mathcal{O}(q^2)$] at all times and at all spatial locations, it is immune to point collisions and is also a solution to the problem when Coulomb collisions are present. The temperature,

$$T(\tau)=T_0\left[c_3(\tau)+q^2\frac{c_2(\tau)c_4(\tau)}{c_1(\tau)}\right]^2, \quad (23)$$

is spatially uniform but oscillates at the rf frequency, $\omega=2$. A similar result was also obtained in our earlier work for the linear field case.[29] The time averaged distribution function can be obtained by doing an average of Eq. (22) over the rf period. The instantaneous density can be obtained by integrating Eq. (22) with respect to velocity,

$$n(x,\tau)=\int_{-\infty}^{\infty}f(x,v,\tau)dv$$
$$=n_0\left[c_3+q^2\frac{c_2c_4}{c_1}\right]$$
$$\times\exp\left[-\beta_0\left\{\frac{1}{2}\left(p+\frac{q^2}{2}\right)\left(\frac{x}{\left[c_1+q^2\dfrac{c_2c_4}{c_3}\right]}\right)^2\right.\right.$$
$$\left.\left.+\frac{q^2\alpha}{4}\left(\frac{x}{\left[c_1+q^2\dfrac{c_2c_4}{c_3}\right]}\right)^4\right\}\right]. \quad (24)$$

As can be seen in the above equation, when space charge effects are taken into account, the density is no longer a Gaussian.

The field induced by the plasma can be obtained by integrating the expression for plasma density, Eq. (24). There is no closed form expression for the result of this integration. However, since we are interested in a region close to the origin, we can expand the exponential in Eq. (24) and integrate the resulting power series keeping only those terms that are important,

$$E(x,\tau)=-4\pi e\int_0^x n(x',\tau)dx'$$
$$\approx-4\pi en_0\left[c_3+q^2\frac{c_2c_4}{c_1}\right]$$
$$\times\left[x-\beta_0\left\{\frac{1}{6}\left(p+\frac{q^2}{2}\right)\frac{x^3}{\left[c_1+q^2\dfrac{c_2c_4}{c_3}\right]^2}\right.\right.$$
$$\left.\left.+\frac{q^2\alpha}{20}\frac{x^5}{\left[c_1+q^2\dfrac{c_2c_4}{c_3}\right]^4}\right\}\right]. \quad (25)$$

In terms of the modified plasma extent, $\bar{x}=1/\sqrt{\beta_0\gamma}$, where $\gamma=0.5p+0.25q^2$; the above equation can be written as

$$E(x,0) = -4\pi e n_0 \bar{x}\left[\frac{x}{\bar{x}} - \frac{x^3}{6\bar{x}^3} - \frac{q^2\alpha}{20\beta_0\gamma^2}\frac{x^5}{\bar{x}^5}\right].$$

If the x^5 term becomes important in the above equation, then our original force equation, Eq. (8), becomes invalid. Thus, the results of this paper are valid when the term containing x^5 in the above equation can be neglected, i.e., when $6q^2\alpha/(20\beta_0\gamma^2) < 1$. This implies

$$\omega_P < 0.8\nu_0. \tag{26}$$

IV. DISCUSSION

A. Space charge effects in rf traps

In experiments on rf traps, one very important issue is the maximum density of plasma that can be trapped for a given value of p_e and q_e. Since the plasma in such traps consists of ions of a single species, it is clear that the plasma is trying to push itself out. For confinement, we must have $p+0.5q^2>0$. This condition translates to $\omega_p < \nu_0 = \sqrt{(p_e+0.5q_e^2)}$. This is the same order of magnitude as the bound prescribed in Eq. (26). Thus, for most rf trap experiments, the x^5 term in Eq. (25) is not very important, hence, our analysis is valid for most practical purposes.

It has been experimentally shown that the choice of $p_e = -0.03$ and $q_e = 0.55$ leads to the most stable configuration in a rf trap and can trap the maximum number of ions.[38] For these values of applied fields, a choice of $\omega_p = \nu_0$ gives a plasma density of the order of 10^5 cm^{-3} for protons in a trap operating at 3 MHz, which is a widely used operating frequency in rf traps. This density is of the same order of magnitude as the maximum possible density of plasma observed in such traps.[38] It must be noted that a value of $q_e = 0.55$ is very high compared to the condition $q_e \ll 1$ for which conventional ponderomotive theory and also our analysis up to $\mathcal{O}(q_e^2)$ holds. Thus, care must be taken while applying theoretical results to actual experiments.

Equation (24) predicts a density that is different from a Gaussian. However, if Eq. (26) is satisfied, then the deviation from a Gaussian is small. As we have shown, when the plasma density exceeds the bound prescribed in Eq. (26), the plasma is very close to the stability boundary beyond which it can no longer be confined. Hence, this explains the reason for which experiments on rf traps observe a Gaussian density.[34]

It is important to note that this maximum density that can be confined also depends on mass. The bound is on plasma frequency, which scales as $\sqrt{n_0/m}$. Thus, for a given maximum ω_p, a larger particle mass results in higher density.

B. Distribution function

Conventionally, the time averaged distribution function for a plasma subject to high frequency electric fields has been assumed to be a function (exponential) of the time averaged ponderomotive Hamiltonian.[16] The idea is that Vlasov's equation preserves f along its orbit hence the proper time averaged distribution for the problem is to require f to be constant on the time averaged trajectories.

Strictly speaking, f is preserved on the exact orbit and the time averaged distribution is the time average of that exact f. However, the exact orbit for a nonautonomous problem has no time-independent invariants and that f is therefore time dependent. As we argued in earlier sections, the only time-independent invariant that can exist in a system with a periodic disturbance is one that is periodic, i.e., an invariant that is time independent if sampled every $2\pi/\omega$. Thus, the only *correct* prescription for a system with a periodic disturbance is an f that is a function of such a periodic invariant. Precisely, such an invariant was obtained up to $\mathcal{O}(q^2)$ in the previous section and Eq. (22) is the distribution based on it.

The only proper time averaged distribution function $\bar{f}$ is therefore the one obtained by time averaging the exact f obtained in the previous section. It is *not* correct to time average the orbits and declare the distribution function to be constant on that time averaged orbit. There are two consequences to the method followed in this paper:

(1) The exact distribution on the actual orbit has been obtained and it is found that, to $\mathcal{O}(q^2)$, the exact distribution is Maxwellian at all times and at all spatial locations. Since this is the case, this solution is also the correct solution [to $\mathcal{O}(q^2)$] for the Vlasov–Boltzmann equation for this problem, where collisions are due to point Coulomb collisions only. This result was obtained earlier for the exactly linear problem and is shown here to be true even when self-consistent effects are taken into account.
(2) The instantaneous temperature is observed to be spatially uniform but oscillates at the rf frequency. This behavior is identical to that observed for the strictly linear problem.[28] There have been conjectures in the literature[2,3] that the plasma temperature should fluctuate at the rf frequency, but this analysis is, to our knowledge, the first proof of these conjectures.

The transformation (x_s, v_s) to (X, V) given below Eq. (18) represents a mapping from the instantaneous orbit to the slow time orbit. Given a stroboscopic orbit that is a closed curve, there is always a mapping. This mapping can be expanded to the desired order in x_s and v_s.

There are many such transformations from (x_s, v_s) to slow time variables (X, V). This is because for different initial points on the instantaneous orbit, different stroboscopic curves are obtained. If one of them lies on a closed curve, then all lie on closed curves. However, only the orbit starting with $[x_s(0), v_s(0)]$ is related to the ponderomotive orbit via a scaling. For the $\mathcal{O}(q^2)$ analysis done here, this map is a linear map of the form

$$\begin{pmatrix} x_s \\ v_s \end{pmatrix} = \begin{pmatrix} R_{11} & qR_{12} \\ qR_{21} & R_{22} \end{pmatrix}\begin{pmatrix} x_s(0) \\ v_s(0) \end{pmatrix},$$

hence the time-dependent invariant is quadratic in velocity at all points on the orbit. This powerful result is what makes this distribution immune to collisions as mentioned above.

When we proceed to higher order, we still have a time-dependent invariant and a time-independent stroboscopic

curve. It is also known that the ponderomotive energy is quadratic in velocity asymptotically.[12] The issue is whether the detailed distribution function is Maxwellian or not at all instants of time. As seen from the transformation above, x_s and v_s get mixed up at the next higher order. Hence, a nonlinearity in space in the form of $\phi_P(x)$ appears in the form of a nonquadratic velocity dependence of the invariant. Thus, to higher order, the distribution function *cannot* be Maxwellian at all points in time. However, it is possible that it is Maxwellian at stroboscopic times, since higher order averaging theory demonstrated this for the ponderomotive Hamiltonian. It is also clear that the higher-order accurate distribution function is not immune to collisions in the way that the $\mathcal{O}(q^2)$ distribution function is immune. Thus, this opens a channel of relaxation of plasmas under the influence of an rf field. The other channel, already discussed in our previous paper,[28] is if more than one species is present in the plasma. Even in linear theory, multiple species systems relax in the presence of collisions.

In this treatment, we have shown that, to the lowest order in the plasma response, the distribution function is a Maxwellian. This was possible because of two reasons. First, the ponderomotive Hamiltonian is quadratic in velocity. Second, the stroboscopic curve could be scaled to get the time averaged ponderomotive orbit and this scaling depends only on the field parameters and not the initial conditions of the particle. For the case where the rf field itself is spatially nonlinear, the first statement is still valid and the stroboscopic orbit can also be approximately scaled to the ponderomotive orbit. However, this scaling now depends on the oscillation amplitude, A. Thus, when we solve the energy equation for A and substitute it back in the expression for the stroboscopic level curve, the term in v will no longer be quadratic. Thus, for spatially nonlinear rf fields, the distribution function is non-Maxwellian even for the lowest order of nonlinearity.

C. Time averaged distribution function

The correct time averaged distribution function is of the form

$$\bar{f}(x,v) = \frac{\omega}{2\pi}\int_{-\pi/\omega}^{\pi/\omega} f(x,v,\tau)d\tau, \tag{27}$$

where $f(x,v,\tau)$ is given by Eq. (22). As discussed in the previous section, the distribution function, $f(x,v,\tau)$ is constant on the detailed orbit and not on the time averaged orbit. Figure 4 makes it clear that the excursions in velocity *are not small*. Indeed, they are as large as the time averaged velocity itself. Thus, a time average of the detailed distribution function cannot be replaced by a distribution function that is constant on the time averaged orbits.

The time averaged distribution function for such problems was obtained by Krapchev.[9] In his analysis, Krapchev obtained the distribution function by solving for the steady state solution of the Vlasov equation directly. The orbits obtained in this paper are the characteristics of that equation. Krapchev used the idea that the distribution function does not see the slow frequency at all, expanded f as a Fourier series in the rf frequency, and also made certain simplifying assumptions to obtain the time averaged solution.

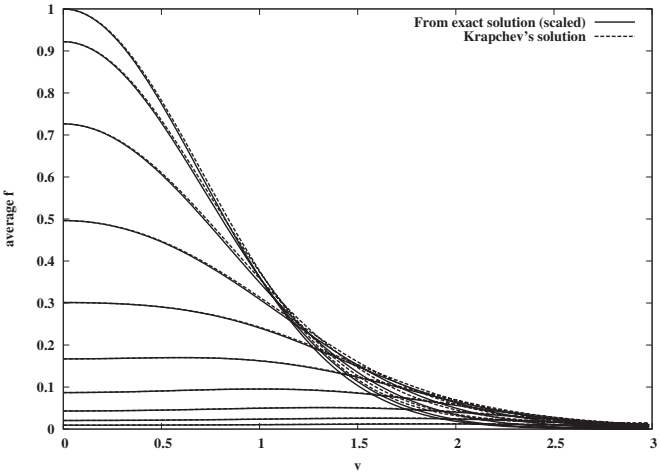

FIG. 4. This is a plot of the time averaged distribution function at different spatial locations. The solid line is obtained from a numerical integration of Eq. (22) and the dashed lines are the ones given in the work of Krapchev (Ref. 9) and are normalized and scaled. As can be seen, the curves cease to be monotonic after a certain threshold in x.

Equation (27) was numerically evaluated and compared with the analytical results obtained by Krapchev for the case of $p=0$ and $\alpha=0$. Figure 4 shows the time averaged distribution function of the plasma as a function of velocity. Each curve in the figure corresponds to a different spatial location separated by $0.2\bar{x}$. The solid curves are the result (normalized and scaled) of numerical integration in Eq. (27) and the dashed lines are the result obtained by Krapchev. As can be seen, at about $x=\bar{x}$, the time averaged distribution function ceases to be monotonic in velocity and becomes double humped. This suggests the presence of instabilities in the plasma, but, by using Penrose's criteria, Krapchev concluded that the plasma is stable. The use of Penrose's criterion in the context of rf plasmas is debatable. The solution obtained by Krapchev does not satisfy the time averaged Vlasov equation, which would yield a Maxwellian distribution confined by a ponderomotive potential. Thus, there is no time-independent kinetic equation whose equilibrium yielded the double humped distribution obtained for $x>\bar{x}$. This being the case, it is not clear how Penrose's criterion is applicable.

In this analysis, we have shown that though the time averaged distribution function is double humped for these spatial locations; the exact time varying distribution function in Eq. (22) is a single humped global Maxwellian at all instants of time. It is quite reasonable, therefore, to believe that the plasma will be stable to small perturbations. Even this, however, is not a proof. There is a source of power in the external rf field and there might well be a fluctuation that could tap into that field and grow.

Krapchev's analysis began with the assumptions that $v\nabla f/\omega f \ll 1$ and that the time averaged plasma distribution is a perturbed Maxwellian. He assumed that response at the nth rf harmonic was of the order of $\mathcal{O}(q^n)$. A consequence of this assumption was that the time averaged distribution function became an even function of q. He used this to obtain a

power series for the response and summed up the series for $\bar{f}$ to infinity by means of a conjecture that the correction of the order of $\mathcal{O}(q^{2n})$ took the form of a Laguerre polynomial of the order of n.

There are several problems with Krapchev's approach. The response at $\mathcal{O}(q)$ is usually much stronger than the response at dc, which is of $\mathcal{O}(q^2)$ since it is related to the ponderomotive potential. Also, as mentioned above, double humped, strongly non-Maxwellian solutions are predicted by this theory, which is not consistent with the perturbative approach. It is quite surprising that these findings are validated by the orbit calculations carried out in this paper. It is our conjecture that his summing up all the higher order corrections to obtain an analytic result extended the validity of his analysis beyond that of his perturbation analysis.

Krapchev's expressions for $\bar{f}$ and $\bar{n}$, if correct, should agree even with the expressions for the response of the plasma to an exactly linear rf field. However, the time averaged density has been shown in our previous paper[28] to be

$$\bar{n}(x) = n_0\left(1 - \frac{q}{2} - \frac{\beta_0}{2}\frac{q^3x^3}{2} + \mathcal{O}(q^2)\right)\exp\left[-\frac{\beta_0}{2}\frac{q^2x^2}{2}\right],$$

which is different from Krapchev's result, reproduced below,

$$\bar{n} = n_0 \exp\left[-\frac{\beta_0}{2}\frac{q^2x^2}{2}\right].$$

Clearly, our expression has odd powers of q, whereas Krapchev's expression implicitly requires the density to be an even function of q. The differences between the two expressions could be interpreted as the difference between the steady state distribution in oscillation center coordinates and the distribution resulting from an initial value problem.

Krapchev's analysis showed the temperature to be spatially nonuniform. However, an exact analysis in this work shows that though the temperature oscillates in time, it is spatially uniform. Krapchev obtained a spatially nonuniform temperature because he used the time averaged distribution function to define temperature. However, this is not correct, since temperature can only be defined for thermodynamic states. In the current problem, the system does go through a sequence of thermodynamic states, but these are continuously oscillating in time. Thus the system cannot be characterized by a single temperature.

It should be noted that the analysis in this paper is self-consistent only for $x \leq \bar{x}$, since the error function has been approximated by a cubic to derive that response. However, the orbits, distribution function, and density for a cubic electric field that have been calculated are valid for a much larger range. Assuming that the validity of these expressions is at least up to where the cubic term competes with the linear term, the calculations are valid as long as

$$\frac{A^2}{376\bar{x}^2}\frac{\nu_0^2}{\nu_0^2 + 0.75q^2\alpha A^2} < 1,$$

which roughly translates to $A < 20\bar{x}$. This bound was verified numerically and the analytic expressions obtained here agree with numerics up to this value of $A \approx x_{\max}(1+0.5q)$. Beyond these values, we see islands forming, as seen in Fig. 1. Though the above comparison has been done for the case when $p=0=\alpha$, the results are qualitatively valid even when $p \neq 0$ and $\alpha \neq 0$.

D. Time averaging and Poincare map

A comparative study of the time averaging method and the Poincare map was done by Hadjidemetriou.[39] As stated in the paper by Hadjidemetriou, the main shortcoming of Poincare map is that, though it accurately describes a dynamical system, it is purely a numerical method. When the orbits are chaotic, averaging methods can play no role in further investigation and Poincare maps are the only way to study dynamics. However it was argued that where the Poincare map leads to closed curves, there averaging methods could lead to a good analytical understanding of the behavior of the solutions. The time averaging methods are very useful because solving the time averaged Hamiltonian is much easier than solving the exact time varying equation. However, as we have shown in this paper, averaging methods applied directly to a time varying Hamiltonian have some important shortcomings. One shortcoming is that the initial condition corresponding to the time averaged Hamiltonian is not the actual initial condition for a particle orbit. To predict this corresponding initial condition for the time averaged Hamiltonian, one has to solve the exact time varying equation. Though this limitation does not dispose of the utility of time averaging methods, it is nevertheless a handicap.

If we are interested in obtaining expressions for the distribution function, it seems mandatory to make efforts toward obtaining an ω-invariant energy expression as has been done in Eq. (20). Thus, there is also an analytical thinking associated with the numerical methods of Poincare maps. Obtaining these ω-invariant energy expressions is, however, not a simple thing. To obtain the ω-invariant energy expression for a given force equation, it is important to obtain analytic expressions for the invariants corresponding to the stroboscopic level curves obtained by fixed-time sampling of the particle orbits. In an earlier work,[40] efforts were made to come up with a scheme (numerical fit) to obtain analytic expressions for the stroboscopic map for orbits corresponding to a given equation of motion. We would like to stress that though it is not very difficult to obtain analytic expressions that would numerically fit to stroboscopic plots, absence of numerically significant errors does not guarantee the correctness of the expression. As we have shown in Eq. (16), it is possible to define a "time" on the stroboscopic plots. Putting $\tau=0$ in Eq. (16) leads to a scaled version of the same orbit expressions, Eq. (14), as that predicted by time averaged ponderomotive Hamiltonian. Thus, there seems to be some dynamical structure behind the stroboscopic plots (with a continuous time defined on these curves) and sufficient care must be taken while obtaining the corresponding ω-invariant energy expressions.

V. CONCLUSIONS

In this work, plasma response to an electrostatic field, which is a superposition of nonlinear dc and linear rf field, has been studied. The expressions for particle orbits, Eq. (9), corresponding to the force equation, Eq. (8), are perturbatively solved for. These solutions are then time averaged and the resulting time averaged orbits, Eq. (12), are compared to the predictions of conventional ponderomotive theory. It is found that the expression for the time averaged particle orbit, Eq. (12), obtained from the exact Hamiltonian is the same as the orbit predicted by time averaged ponderomotive Hamiltonian, Eq. (13), in the limit $\nu \rightarrow 0$. However, as is well known in the context of oscillation center theories, for ponderomotive theory to be able to predict the time averaged orbit, we need to know the ponderomotive initial conditions, $x_p(0)$, $v_p(0)$ corresponding to the actual initial conditions, x_0, v_0. For this, we need to perturbatively solve the exact equation, Eq. (8).

It has been shown that the idea of time averaged distribution function is different from that of obtaining time averaged particle orbits or time averaged Hamiltonian. The time averaged distribution function is not constant on the time averaged particle orbits in phase space. The ω-invariant distribution function, Eq. (22), is a function of the resultant ω-invariant energy expression, Eq. (20). Thus, the time average of this ω-invariant distribution function is different from the exponential of the time averaged ponderomotive Hamiltonian, Eq. (13). The temperature is also found to periodically oscillate with time but is constant with space. However, the plasma has been found to be a Maxwellian only up to $\mathcal{O}(q^2)$. This could be a possible reason for the observed heating in rf traps.

It was shown by Krapchev that the time averaged distribution function is nonmonotonic with respect to velocity beyond a certain threshold in space. We validated his results by carrying out a time average of the exact time varying distribution function. The limitations of Krapchev's work have also been brought out.

Apart from theoretical relevance, the results obtained in this work are very important from the experimental point of view. We have shown that the condition, Eq. (26), where the plasma density deviates from being a Gaussian is very close to the maximum plasma density that has been experimentally observed to be trapped in a rf trap. Also, the maximum plasma density that can be confined in such traps has been shown to linearly scale with the mass of the confined ions.

[1] W. Paul, Rev. Mod. Phys. **62**, 531 (1990).
[2] I. Siemers, R. Blatt, Th. Sauter, and W. Neuhauser, Phys. Rev. A **38**, 5121 (1988).
[3] F. Vedel, Int. J. Mass Spectrom. Ion Process. **106**, 33 (1991).
[4] J. Walz, I. Siemers, M. Schubert, W. Neuhauser, R. Blatt, and E. Teloy, Phys. Rev. A **50**, 4122 (1994).
[5] D. J. Berkeland, Rev. Sci. Instrum. **73**, 2856 (2002).
[6] R. C. Davidson, H. Qin, and G. Shvets, Phys. Plasmas **7**, 1020 (2000).
[7] D. R. Nicholson, *Introduction to Plasma Theory* (Wiley, New York, 1983), p. 31.
[8] J. R. Cary and A. N. Kaufman, Phys. Fluids **24**, 1238 (1981).
[9] V. B. Krapchev, Phys. Rev. Lett. **42**, 497 (1979).
[10] R. G. Littlejohn, Phys. Fluids **24**, 1730 (1981).
[11] B. M. Lamb and G. J. Morales, Phys. Fluids **26**, 3488 (1983).
[12] J. Guckenheimer and P. Holmes, *Nonlinear Oscillations, Dynamical Systems, and Bifurcations of Vector Fields* (Springer-Verlag, New York, 1983), p. 166.
[13] J. A. Sanders, Celest. Mech. **28**, 171 (1982).
[14] M. Levi, Physica D **132**, 150 (1999).
[15] I. A. Mitropolsky, Int. J. Non-linear Mech. **2**, 69 (1967).
[16] K. Avinash, A. K. Agarwal, M. R. Jana, A. Sen, and P. K. Kaw, Phys. Plasmas **2**, 3569 (1995).
[17] C. Joshi, Phys. Plasmas **14**, 055501 (2007).
[18] W. Lu, C. Huang, M. Zhou, M. Tzoufras, F. S. Tsung, W. B. Mori, and T. Katsouleas, Phys. Plasmas **13**, 056709 (2006).
[19] P. Mora and T. M. Antonsen, Jr., Phys. Plasmas **4**, 217 (1997).
[20] V. E. Zakharov, Sov. Phys. JETP **35**, 908 (1972).
[21] J. D. Prestage, G. J. Dick, and L. Maleki, J. Appl. Phys. **66**, 1013 (1989).
[22] J. C. Schwartz, M. W. Senko, and J. E. P. Syka, J. Am. Soc. Mass Spectrom. **13**, 659 (2002).
[23] G. Z. Li, R. Poggiani, G. Testera, G. Torelli, and G. Werth, Hyperfine Interact. **76**, 343 (1993).
[24] J. M. Finn, R. Nebel, A. Glasser, and H. R. Lewis, Phys. Plasmas **4**, 1238 (1997).
[25] J. Walz, S. B. Ross, C. Zimmermann, L. Ricci, M. Prevedelli, and T. W. Hansch, Hyperfine Interact. **100**, 133 (1996).
[26] J. F. J. Todd, Mass Spectrom. Rev. **10**, 3 (1991).
[27] A. Steane, Appl. Phys. B: Lasers Opt. **64**, 623 (1997).
[28] K. Shah and H. Ramachandran, Phys. Plasmas **15**, 062303 (2008).
[29] A. J. Lichtenberg and M. A. Lieberman, *Regular and Chaotic Dynamics* (Springer-Verlag, New York, 1991), p. 50.
[30] N. W. McLachlan, Math. Gaz. **35**, 32 (1951).
[31] A. A. Vlasov, J. Phys. (USSR) **9**, 25 (1945).
[32] M. Kruskal, J. Math. Phys. **3**, 806 (1962).
[33] R. Ifflander and G. Werth, Metrologia **13**, 167 (1977).
[34] H. Schaaf, U. Schmeling, and G. Werth, Appl. Phys. (Berlin) **25**, 249 (1981).
[35] N. W. McLachlan, *Theory and Applications of Mathieu Functions* (Oxford University Press, Oxford, 1947).
[36] See EPAPS Document No. E-PHPAEN-16-053906 for Appendices A–D. For more information on EPAPS, see http://www.aip.org/pubservs/epaps.html.
[37] P. Amore and A. Aranda, Phys. Lett. A **316**, 218 (2003).
[38] R. Alheit, C. Hennig, R. Morgenstern, F. Vedel, and G. Werth, Appl. Phys. B: Lasers Opt. **61**, 277 (1995).
[39] J. D. Hadjidemetriou, Nonlinear Phenom. Complex Syst. (Dordrecht, Neth.) **11**, 149 (2008).
[40] W. Eberl, M. Kuchler, A. Hubler, E. Luscher, M. Maurer and P. Meinke, Z. Phys. B: Condens. Matter **68**, 253 (1987).